POLISH POLAR RESEARCH
vol. 35, no. 1, pp. 41–71, 2014 doi: 10.2478/popore-2014-0004

Depositional conditions and petroleum potential of the Middle Triassic Passhatten Member (Bravaisberget Formation), Spitsbergen

Przemysław KARCZ

Państwowy Instytut Geologiczny-Państwowy Instytut Badawczy, ul. Rakowiecka 4, 00-975 Warszawa, Poland <przemyslaw.karcz@pgi.gov.pl>

Instytut Nauk Geologicznych Polskiej Akademii Nauk, ul. Twarda 51/55, 00-818 Warszawa, Poland

Abstract: The Passhatten Member (Anisian–Ladinian) is the most westward exposure of the Middle Triassic sedimentary sequence of Spitsbergen. The member has an average organic carbon of 2.21 wt %. The sediments were deposited in a shallow shelf environment under conditions of high biological productivity stimulated by a well-developed upwelling system and an enhanced nutrient supply from land areas. The high biological productivity caused a high supply of organic particles to the shelf bottom. Decomposition of organic matter initiated oxygen deficiency in the bottom waters; however, bottom water dynamics on the shallow shelf temporarily replenished the oxygen. Consequently, the Passhatten Mb section is bioturbated, even in thick black shale horizons and consists of alternately spaced lithological layers with variable organic carbon content. The organic matter is dominated by type II kerogen with a mixture of strongly altered marine and/or land derived organic matter. Calculated initial hydrogen index values suggest oil-prone organic matter similar to kerogen I and II types. The organic matter is in the upper intermediate stage of thermo-catalytic alteration, close to the cata- and metagenetic boundary. Maturity indicators including Rock-Eval, Maximum Temperature, Organic Matter Transformation Ratio, Residual Carbon content, as well as the volume of methane generated suggest mature to overmature organic matter. Methane potential retained in the black shales sequence is significant. Unexpelled gas is estimated at 395 mcf/ac-ft for the examined section.

Key words: Arctic, Spitsbergen, Middle Triassic, Bravaisberget Formation, depositional conditions, organic carbon, petroleum potential.

Introduction

The Passhatten Member (Anisian–Ladinian in age; Birkenmajer 1977; Mørk *et al.* 1982) is the main lithological horizon of the Bravaisberget Formation and constitutes more than two thirds of the unit's total thickness (Fig. 1). The member

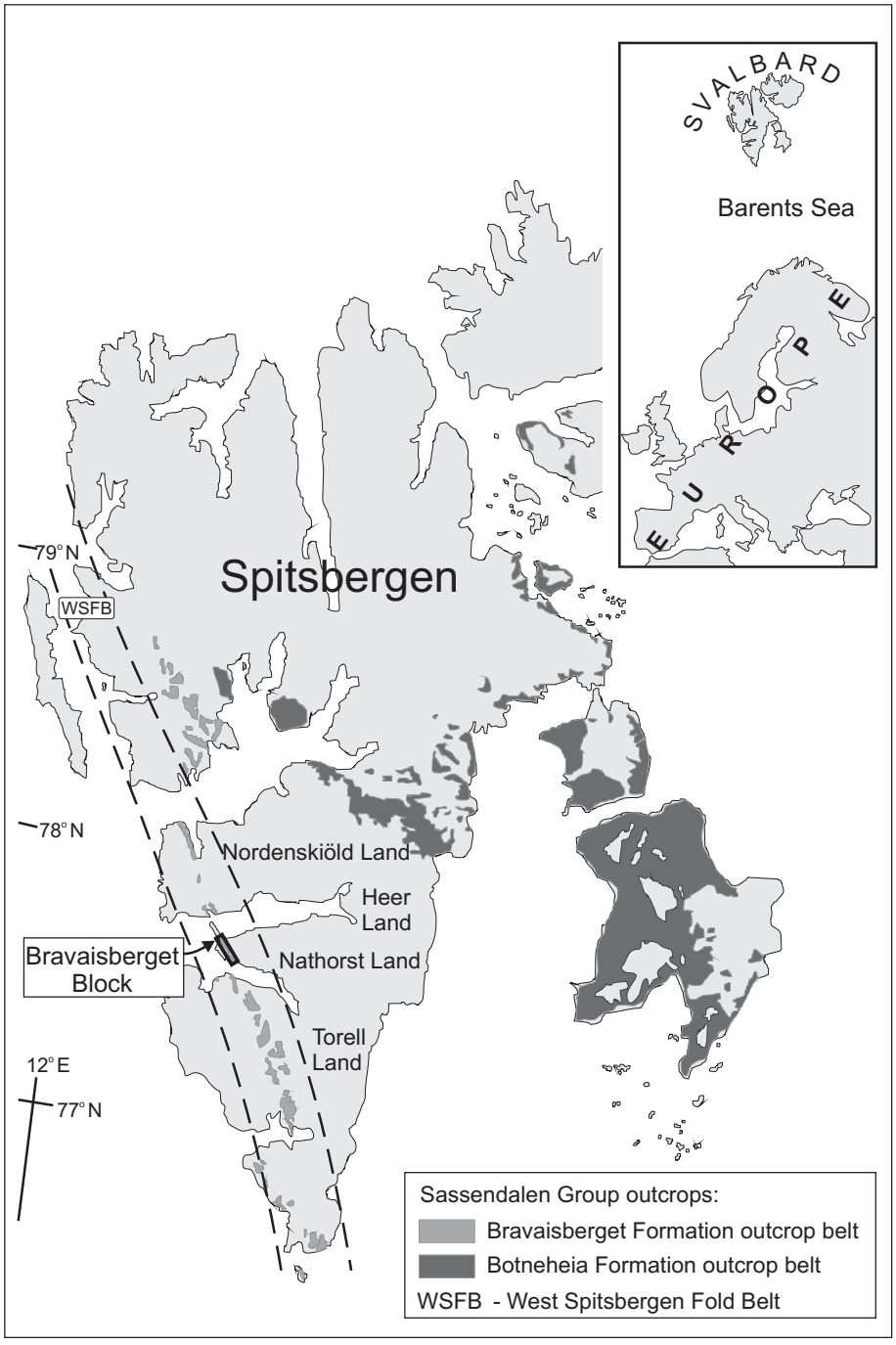

Fig. 1. Sketch map of the Svalbard archipelago showing Triassic outcrop belts of the organic-rich sediments of the Bravaisberget and Botneheia formations (Sassendalen Group; after Dallmann 1999) and the location of the Bravaisberget Block.

stretches along the western Spitsbergen margin and consists of interbedded layers of black shale beds, siltstones and fine-grained phosphorite-bearing sandstones. The black shales are organic-rich mud, silt, and very fissile clay shales deposited in a shallow shelf environment (Birkenmajer 1977; Mørk *et al.* 1982; Krajewski 2000a–c; Krajewski *et al.* 2007; Karcz 2008). The Total Organic Carbon (TOC) ranges from 0.6 to 4.9 wt % (Karcz 2010).

The black shales were deposited on the muddy bottom with fluctuating oxygen levels ranging from euxinic, through dysoxic, to slightly oxic conditions (Krajewski *et al.* 2007). During sediment deposition, intense reworking by bottom currents controlled an oxygenation of the sea floor. Intercalations of black shales and phosphorite-bearing sandstones resulted from sediment deposition under variable oxygen regimes (Mørk and Bromley 2008).

Two transgressive pulses have been recognized in the Passhatten Mb section: the first one, early Anisian in age, marks the boundary of the Passhatten Mb with the underlying Tvillingodden Fm (Mørk *et al.* 1982). The second, late Anisian transgressive pulse marks an internal boundary between sections of distinctive organic carbon content (Karcz 2010). The two transgressive pulses induced biological productivity in the surface waters on the Svalbard shelf and deepened the marine environment. The increased height of the water column caused a probable decrease in the dynamics of both the sedimentary basin and its bottom environments. Consequently, these events enhanced the supply and preservation of organic matter.

Steel and Worsley (1984) and Krajewski (2000a) proposed that the organic-rich sediments of the Triassic shelf environment of Svalbard were deposited under a zone of maximum biological productivity, dominated by a widespread upwelling system with nutrients supplied from adjacent land areas.

Materials and samples

The black shale samples were collected from the Passhatten Mb in the stratotype section of the Bravaisberget Fm located in the western Nathorst Land at Bravaisberget (Fig. 1). The Passhatten Mb in the mentioned above section reaches about 160 meters with 100 meters of black shales, therein.

The samples were collected by K. Birkenmajer, K.P. Krajewski and B. Luks during the expedition of the Polish Academy of Sciences to Spitsbergen in 2002, and subsequently they were made available for PhD dissertation and organic petrological analyses of an author of the article. Presently the samples are housed in the Institute of Geological Sciences, Polish Academy of Sciences, Warszawa, Poland.

Sedimentary features of the black shales vary between individual lithological horizons, from small-scale cross-laminated in the lower part, to planar-laminated internal structure in the upper part. The planar-laminated internal structure is often

accentuated by directional arrangement of calcified fragments of thin-shelled pelecypods (Fig. 2; sample B1-142) and directionally oriented mineral grains.

The main mineral constituent of the examined sedimentary rocks is quartz in the very fine to coarse silt fraction surrounded by illite-dominated mud shale. The average content of quartz is about 23% in the clay and mud shales, increasing up to 40% in silt shale. The quartz grains are dominated by monocrystals rimmed with authigenic quartz. The black shales are mostly dominated by amorphous organic matter occurring usually as organo-clay aggregates in the matrix. Muscovite, biotite, and chlorite occur as subordinate rock components (1–5%). Detrital feldspar and heavy minerals, such as titanite, rutile, tourmaline, zircon, and garnet occur only as accessory content. In general, the size and quantity of the detrital fraction decreases upwards with the exception of the biogenic debris represented by thin-shelled pelecypods, mostly occurring in the upper section of the member. Detrital grains are usually well sorted and poorly rounded with the exception of feldspars.

Among the diagenetic minerals, carbonates, pyrite, quartz, barite, and sphalerite have been recognized. Carbonates are dominated by calcareous micrite and microsparite, usually filling pore spaces in the black shales. The calcareous cement usually replaces biogenic debris and forms pseudo-structures after both siliceous radiolarian tests and sponge spicules. Other types of carbonates in the rocks include dolomite, Fe-dolomite, and negligible amounts of ankerite.

Clay minerals form one of the most frequently occurring components of the black shales. Energy Dispersive Spectroscopy analysis revealed ubiquitous occurrence of detrital and authigenic illite. Clay minerals visible in the whole section of the Passhatten Mb (Fig. 2) form laminas and seams, fill inter-particle pore space, and often coat detrital grains. Dispersed chlorite in the shales occurs as an allogeneic mineral. The lower section of the member is dominated by the co-occurrence of clay and authigenic calcitic and phosphatic cements. The amount of phosphatic cement decreases in the upper section, which is evidently dominated by clay cement. Early-diagenetic pyrite occurs as an accessory mineral in all the analyzed samples as dispersed or concentrated microcrystals and/or (poly)framboids (Karcz 2010). Microcrystals dominate over (poly)framboids in the entire analyzed section. The (poly)framboids content decreases significantly in the upper section. Quartz cement occurs in minor quantities only; it is represented by regeneration rims on detrital quartz grains. Authigenic quartz in the form of rims growing on detrital grains does not fill the pore space.

Fig. 2. Comparison of the most representative thin sections from the lower (samples B1-16 and B1-94) and the upper (sample B1-142) part of the Passhatten Mb. B1-16: winnowed horizon dominated by detrital quartz grains and calcitic cement, mud shale, crossed nicols; B1-94: winnowed and not winnowed horizons in one sample of mud shale, crossed nicols; B1-142: domination of the thin-shelled pelecypods in mud shale, crossed nicols. Q – quartz grains, Pe – euhedral pyrite crystals, Cc – calcitic cement, Wh – winnowed horizon, TsP – thin-shelled pelecypods. →

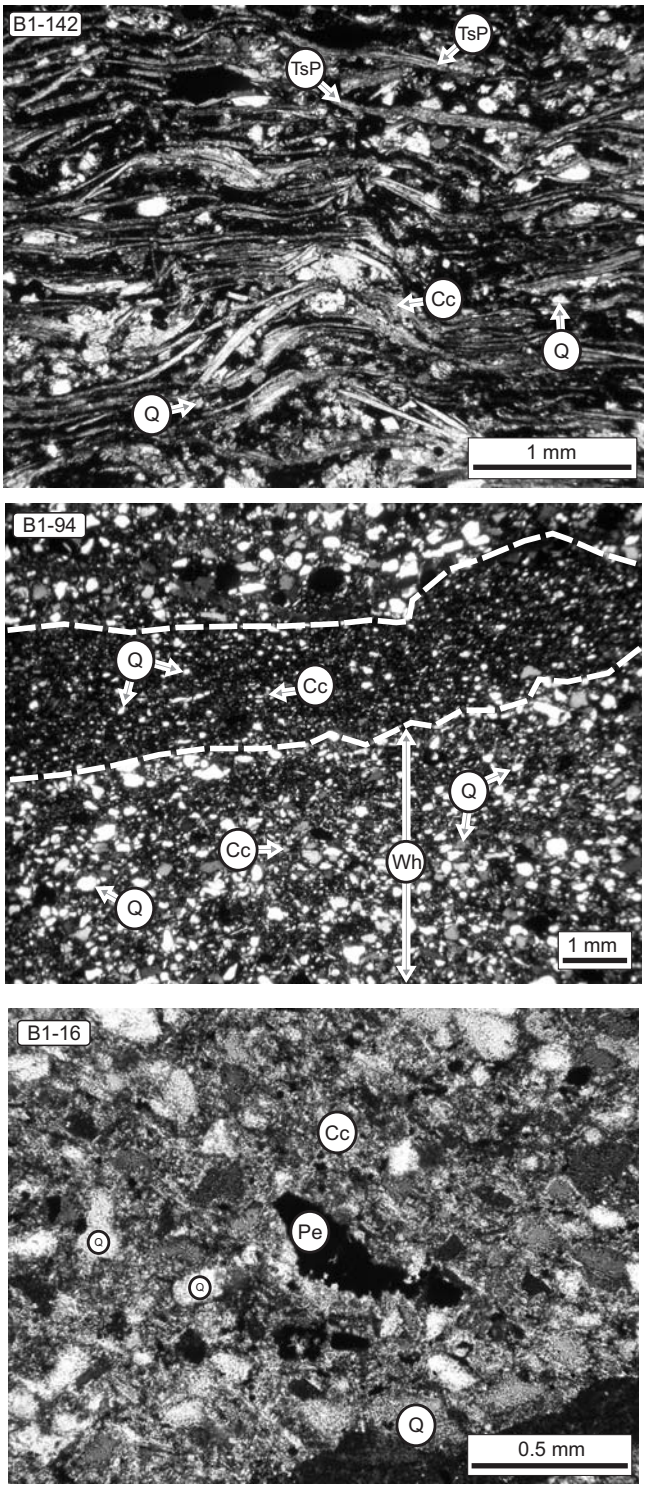
B1-142
TsP
TsP
Cc
Q
Q
1 mm
B1-94
Q
Cc
Q
Cc
Wh
Q
1 mm
B1-16
Cc
Pe
Q
0.5 mm

Bioturbation is abundant in all the studied rock types. Vertical and horizontal bioturbations vary from ~2 to 10 mm. Statistical analysis of bioturbation revealed that these structures are more common in the black shales from the lower, rather than the upper section of the Passhatten Mb.

Methods

Rock Eval pyrolysis measurements were performed in the Oil and Gas Institute in Kraków (Poland) using Rock-Eval 6 apparatus. This technique involves the thermal decomposition of crushed rock in a helium or nitrogen atmosphere (Espitalié *et al.* 1977a, b). The sample is heated to 650°C. Volatile hydrocarbons present in the rock are released at temperatures below 350°C. The amount of free hydrocarbons (S1) thermally liberated from a rock sample at 300°C is measured using a Flame Ionization Detector (FID). As the temperature continues to increase, kerogen breaks down releasing hydrocarbons. Carbon dioxide and water are released at temperatures above 550°C. Carbon dioxide formed at this temperature comes mainly from the thermal decomposition of kerogen, because the majority of carbonates (with the exception of fine-grained siderite) require higher temperatures to decompose. Volatile components released during pyrolysis are separated into two streams. One of them passes through the FID and the graph is registered as peak S2. The hydrocarbons are released from a rock sample during heating in the range of temperature between 300°C and 650°C. Another volatile component released during pyrolysis, *i.e.*, carbon dioxide generated from kerogen, is recorded by a thermal conductivity detector as the S3 peak.

Fifty-seven black shale samples covering the whole section of the Passhatten Mb in regular intervals were pyrolyzed as part of the Rock Eval measurements (Karcz 2008).

Petrographic analyses were carried out on 21 black shale samples (Karcz 2009). The samples were coated with an epoxy resin and polished. Then, all these polished sections were examined with a Zeiss Axioskop microscope with microphotometer, using reflected white light and under fluorescence in oil immersion. Vitrinite reflectance measurements included at least 70 random measurements of each polished section. International Committee for Coal Petrology (ICCP) nomenclature and classification has been applied in this paper according to ICCP (1998). The maceral composition of organic matter has been estimated in regularly distributed lines, with total observations of a few hundreds.

The estimations of initial values of different geochemical parameters were applied according to procedures described in Jarvie *et al.* (2007). The method allows the estimation of the initial values of many geochemical parameters, such as hydrogen, and productive indexes (HI_o, PI_o), and total organic carbon (TOC_o) as well.

It is also possible to calculate the Transformation Ratio (TRHI) based on present day data and initial hydrogen indexes (HI_{pd}, HI_o).

It is possible to calculate the initial hydrogen index data based on the maceral percentages from visual kerogen assessments and assigned kerogen-type average values. Using the following equation enables the appropriate computation:

$$HI_o = \left(\frac{\%typeI}{100} \times 750\right) + \left(\frac{\%typeII}{100} \times 450\right) + \left(\frac{\%typeIII}{100} \times 125\right) + \left(\frac{\%typeIV}{100} \times 50\right) \quad (1)$$

The TRHI in terms of the extent of organic matter conversion can be determined based on the following equation:

$$TRHI = 1 - \frac{HI_{pd}\left[1200 - HI_o(1 - PI_o)\right]}{HI_o\left[1200 - HI_{pd}(1 - PI_{pd})\right]} \quad (2)$$

The TRHI parameter depends on changes of HI between the initial and present day values. PI_{pd} is the present day Production Index, whilst PI_o is the initial Production Index resulting from the equation of Peters *et al.* (2006), where PI_o = 0.02 to PI_{pd}.

The TOC_o can be determined using equation 3, which requires HI_{pd}, HI_o, and TRHI data:

$$TOC_o = \frac{HI_{pd}\left(\frac{TOC_{pd}}{1+k}\right)(83.33)}{\left[HI_o(1 - TRHI)\left(83.33 - \left(\frac{TOC_{pd}}{1+k}\right)\right)\right] + \left[HI_{pd}\left(\frac{TOC_{pd}}{1+k}\right)\right]} \quad (3)$$

The *k* is a correction factor related to the residual organic carbon computed from the formula TRHI · RC, where RC is the present day Residual Carbon (Burnham 1989).

Generally, the symbol "pd" has been used in the terms for the present day values, *i.e.*, after hydrocarbon generation, as opposed to the symbol "o" which means the initial, primary values. The latter symbol is believed to represent values prior to hydrocarbon generation.

The presented basic equations from 1 to 3 are necessary for the computation of the preliminary resources. The resources data were calculated according to two procedures described in Schmoker (1994) and Jarvie *et al.* (2007). The first method is based on relationships between a certain volume of rock unit, shales density, TOC, and HI_o values. The second method is based on the relationships between maceral percentages, TRHI, and TOC_o, which allows an estimation of the expelled and unexpelled gaseous hydrocarbons.

Results

The data from the Rock Eval analysis include records measured during the pyrolysis and also data reprocessed as a result of mathematical calculations. Among the first group are: TOC, Tmax – Maximum Temperature, S1, S2, S3, HI, OI – Oxygen Index, RC, PC – Productive Carbon. Mathematically reprocessed data include: PI – [S1/(S1+S2)], PP – Petroleum Potential (S1+S2), HC – petroleum potential expressed in units of ppm, RC – TOC – percentage content of residual carbon in total organic carbon.

TOC_{pd} values fluctuate between 0.65 and 4.92 wt % (Table 1). The lithological interval between samples B1-12–104 is characterized by lower TOC_{pd} values of 0.65 to 3.17%, whilst the upper interval has typical TOC_{pd} values up to 4.92%. TOC_o values range between 0.96 and 5.02% (Table 2). The TOC_o values correlate fairly well with TOC_{pd} (Fig. 3). The difference between TOC_o and TOC_{pd} fluctuates between 0.05 and 1.10% (average 0.49%).

The obtained Tmax values fall in the range between 449°C and 467°C and show a clear increase with depth.

S1, S2, and S3 values oscillate between 0.14–0.92, 0.55–5.38 mgHC/gRock, and 0.20–0.64 $mgCO_2$/gRock, respectively (Table 1).

HI_{pd} values range between 55 and 122 (mgHC/gTOC). The lithological horizon between samples B1-12–48 is characterized by low HI_{pd} values (55–99 mgHC/gTOC), whilst within the overlying interval (B1-63–146), HI_{pd} values are in the range between 71 and 122 (mgHC/gTOC; Table 1). Generally, HI_{pd} values increase upwards in the Passhatten section. HI_o values fall in the range between 366 and 653 (mgHC/gTOC; Table 2). The values correlate negatively with HI_{pd} and show a decreasing trend towards the top of the section.

OI_{pd} is in the range from 7 to 72 ($mgCO_2$/gTOC). There are also some values exceeding 30 ($mgCO_2$/gTOC) and most of these are in the lower section of the Passhatten Mb (B1-12–104).

RC_{pd} and PC_{pd} values are in the range between 0.57–4.38 and 0.07–0.54%, respectively.

PI_{pd}, PP_{pd}, and HC are characterized by the following ranges of values, respectively: 0.08–0.28 (mgHC/gTOC), 0.69–6.30 (kgHC/tRock), and 690–6300 (ppm). PI_{pd} and PP_{pd} data show a downwards and upwards increase, respectively (Table 1).

RC_{pd} in TOC_{pd} values are dominated by relatively high values between 85 and 93%. The distribution of the data shows an increase towards the bottom of the member.

All maceral groups are dominated by the occurrence of the smallest organic particles of vitrodetrinite, inetrodetrinite, and liptodetrinite. Other types of macerals, such as semifuzinite and alginite occur as accessories. The content of vitrinite as a percentage volume of the maceral population fluctuates between 6% and 40% and the maceral shows a trend of a gradual decrease upwards towards the top of the

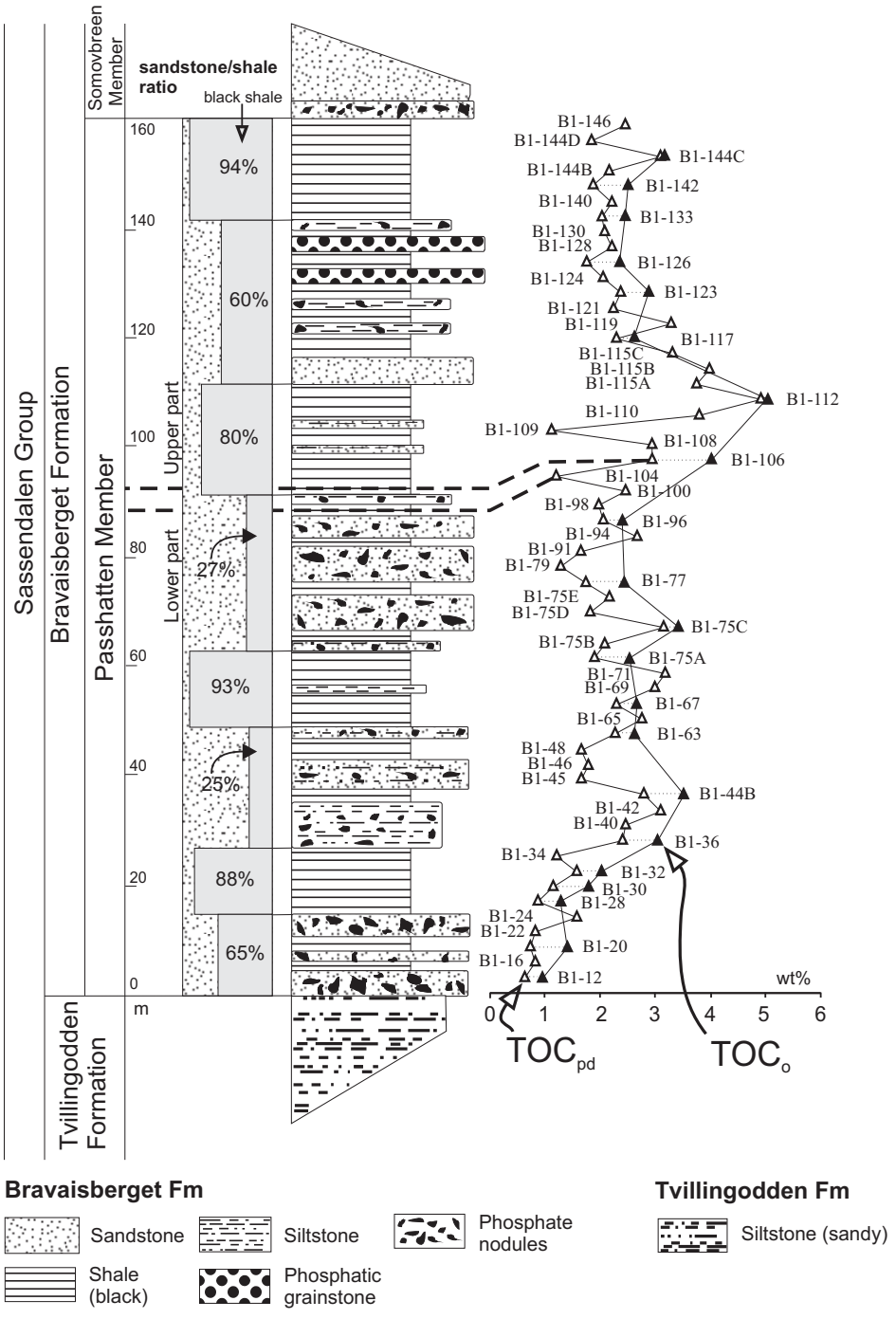

Fig. 3. Simplified section of the Passhatten Mb against the plots of the sandstone/shale ratio and a visible good correlation between TOC_{pd} and TOC_o. Profile and sandstone/shale ratio after Krajewski *et al.* (2007).

Table 1

Rock Eval pyrolysis data from samples of the Passhatten Mb.

Samples	TOC_{pd}	T_{max}	$S1_{pd}$	$S2_{pd}$	$S3_{pd}$	HI_{pd}	OI_{pd}	RC_{pd}	PC_{pd}	PI_{pd}	PP_{pd}	HC	Rc_{pd}-TOC_{pd}
	wt%	°C	mgHC/gRock	$mgCO_2$/gRock	mgHC/gTOC	$mgCO_2$/gTOC	%	%	mgHC/gRock	kgHC/tRock	ppm	%	
B1-146	2.44	457	0.53	2.77	0.30	114	12	2.15	0.29	0.16	3.30	3300	88
B1-144 D	1.85	459	0.42	1.84	0.31	99	17	1.64	0.21	0.19	2.26	2260	89
B1-144 C	3.09	461	0.76	3.27	0.32	106	10	2.73	0.36	0.19	4.03	4030	88
B1-144 B	2.16	453	0.56	2.20	0.29	102	13	1.92	0.24	0.20	2.76	2760	89
B1-142	1.88	457	0.39	1.69	0.23	90	12	1.69	0.19	0.19	2.08	2080	90
B1-140	2.22	458	0.45	2.23	0.51	100	23	1.96	0.26	0.17	2.68	2680	88
B1-133	2.03	459	0.38	2.18	0.34	107	17	1.80	0.23	0.15	2.56	2560	89
B1-130	2.08	459	0.44	2.22	0.51	107	25	1.83	0.25	0.17	2.66	2660	88
B1-128	2.21	454	0.34	2.16	0.33	98	15	1.97	0.24	0.14	2.50	2500	89
B1-126	1.76	449	0.27	1.25	0.64	71	36	1.60	0.16	0.18	1.52	1520	91
B1-124	2.06	457	0.49	2.06	0.32	100	16	1.83	0.23	0.19	2.55	2550	89
B1-123	2.37	455	0.66	2.21	0.45	93	19	2.11	0.26	0.23	2.87	2870	89
B1-121	2.24	456	0.65	2.24	0.27	100	12	1.99	0.25	0.22	2.89	2890	89
B1-119	3.28	457	0.91	3.44	0.37	105	11	2.90	0.38	0.21	4.35	4350	88
B1-117	2.29	456	0.42	2.33	0.58	102	25	2.03	0.26	0.15	2.75	2750	89
B1-115 C	3.31	458	0.37	3.70	0.37	112	11	2.93	0.38	0.09	4.07	4070	89
B1-115 B	3.99	462	0.53	4.36	0.52	109	13	3.56	0.43	0.11	4.89	4890	89
B1-115 A	3.74	462	0.67	4.22	0.44	113	12	3.30	0.44	0.14	4.89	4890	88
B1-112	4.92	460	0.92	5.38	0.35	109	7	4.38	0.54	0.15	6.30	6300	89
B1-110	3.79	460	0.64	3.98	0.59	105	16	3.37	0.42	0.14	4.62	4620	89
B1-109	1.12	457	0.28	1.05	0.31	94	28	0.99	0.13	0.21	1.33	1330	88
B1-108	2.93	459	0.51	3.23	0.63	110	22	2.58	0.35	0.14	3.74	3740	88
B1-106	2.93	459	0.51	3.23	0.63	110	22	2.58	0.35	0.14	3.74	3740	88
B1-104	1.20	461	0.38	1.36	0.31	113	26	1.04	0.16	0.22	1.74	1740	87
B1-100	2.46	462	0.34	2.20	0.48	89	20	2.23	0.23	0.13	2.54	2540	91
B1-98	1.97	459	0.21	1.94	0.33	98	17	1.77	0.20	0.10	2.15	2150	90
B1-96	2.07	459	0.36	2.02	0.32	98	15	1.86	0.21	0.15	2.38	2380	90
B1-94	2.67	461	0.55	2.51	0.64	94	24	2.38	0.29	0.18	3.06	3060	89
B1-91	1.67	462	0.33	1.48	0.44	89	26	1.50	0.17	0.18	1.81	1810	90
B1-79	1.28	462	0.59	1.56	0.33	122	26	1.09	0.19	0.27	2.15	2150	85
B1-77	1.73	460	0.48	1.64	0.29	95	17	1.54	0.19	0.23	2.12	2120	89
B1-75 E	2.16	463	0.43	2.17	0.32	100	15	1.92	0.24	0.17	2.60	2600	89
B1-75 D	1.83	457	0.18	1.59	0.38	87	21	1.66	0.17	0.10	1.77	1770	91
B1-75 C	3.15	463	0.73	3.55	0.28	113	9	2.78	0.37	0.17	4.28	4280	88
B1-75 B	2.08	461	0.44	1.93	0.31	93	15	1.87	0.21	0.19	2.37	2370	90
B1-75 A	1.90	459	0.28	1.86	0.40	98	21	1.70	0.20	0.13	2.14	2140	89
B1-71	3.17	464	0.65	3.37	0.28	106	9	2.82	0.35	0.16	4.02	4020	89
B1-69	3.00	465	0.47	2.59	0.39	86	13	2.72	0.28	0.15	3.06	3060	91
B1-67	2.29	463	0.64	2.42	0.40	106	17	2.01	0.28	0.21	3.06	3060	88
B1-65	2.76	460	0.72	3.32	0.23	120	8	2.41	0.35	0.18	4.04	4040	87
B1-63	2.27	460	0.67	2.35	0.34	104	15	2.00	0.27	0.22	3.02	3020	88
B1-48	1.67	467	0.25	1.31	0.35	78	21	1.52	0.15	0.16	1.56	1560	91
B1-46	1.79	462	0.26	0.99	0.47	55	26	1.66	0.13	0.21	1.25	1250	93
B1-45	1.66	458	0.16	1.28	0.40	77	24	1.51	0.15	0.11	1.44	1440	91
B1-44 B	2.81	461	0.30	2.18	0.51	78	18	2.58	0.23	0.12	2.48	2480	92
B1-42	3.10	462	0.27	2.53	0.55	82	18	2.84	0.26	0.10	2.80	2800	92
B1-40	2.47	459	0.17	1.84	0.64	74	26	2.26	0.21	0.08	2.01	2010	91
B1-36	2.41	460	0.21	2.09	0.39	87	16	2.20	0.21	0.09	2.30	2300	91
B1-34	1.21	461	0.20	1.00	0.40	83	33	1.09	0.12	0.17	1.20	1200	90
B1-32	1.59	462	0.36	1.58	0.27	99	17	1.41	0.18	0.19	1.94	1940	89
B1-30	1.16	462	0.29	0.96	0.31	83	27	1.04	0.12	0.23	1.25	1250	90
B1-28	0.87	456	0.21	0.55	0.20	63	23	0.80	0.07	0.28	0.76	760	92
B1-24	1.57	464	0.33	1.29	0.31	82	20	1.42	0.15	0.20	1.62	1620	90
B1-22	0.84	461	0.29	0.73	0.40	87	48	0.74	0.10	0.28	1.02	1020	88
B1-20	0.74	462	0.14	0.55	0.21	74	28	0.67	0.07	0.20	0.69	690	91
B1-16	0.82	458	0.15	0.60	0.35	73	43	0.74	0.08	0.20	0.75	750	90
B1-12	0.65	456	0.15	0.62	0.47	95	72	0.57	0.08	0.19	0.77	770	88

Passhatten Mb (Table 2, Fig. 4). The content of inertodetrinite falls in the range from 20% and 80% and the maceral shows a trend of increase upwards towards the top of the member. The content of liptinite range is between 0% and 74% and is similar to the vitrinite trend.

The average vitrinite reflectance values range from 0.90% to 1.28% R_o (Table 2). The average R_o values show a trend of a slight decrease with depth, in contrast

Table 2

Results of the organic petrology, vitrinite reflectance, transformation ratio (TRHI), initial organic carbon and hydrogen index (TOC_o; HI_o) and volume of generated methane from samples of the Passhatten Mb.

Samples	Vitrinite	Inertinite	Liptinite	Ro			TR	TOC_o	HI_o	Volume of generated methane
				Min	AVG	Max				
	[%]	[%]	[%]	[%]	[%]	[%]	[%]	[wt%]	[mgHC/gTOC]	[%]
B1 - 144C	26	74	0	0.62	1.28	1.97	77	3.14	366	95
B1 - 142	21	41	38	0.75	1.14	1.54	88	2.51	496	94
B1 - 133	9	80	11	0.98	1.25	1.57	83	2.47	454	95
B1 - 126	10	74	16	0.72	1.13	1.73	89	2.34	466	94
B1 - 123	10	74	16	0.69	1.11	1.44	86	2.88	466	94
B1 - 117	28	52	20	0.70	1.03	1.40	82	2.63	419	93
B1 - 112	29	29	42	0.86	1.19	1.94	84	5.02	482	95
B1 - 106	6	34	60	1.01	1.11	1.43	89	4.03	611	94
B1 - 96	33	50	17	0.71	0.95	1.16	81	2.40	394	93
B1 - 77	13	43	43	0.70	1.01	1.53	89	2.42	532	93
B1 - 75C	40	20	40	0.83	1.20	1.52	81	3.41	440	95
B1 - 75A	17	47	36	1.00	1.17	1.52	86	2.53	503	95
B1 - 67	29	43	29	0.64	0.90	1.48	83	2.67	447	92
B1 - 63	28	45	26	1.10	1.23	1.50	83	2.62	433	95
B1 - 44B	22	44	33	0.72	0.94	1.40	88	3.54	473	93
B1 - 36	30	33	37	0.78	1.06	1.34	86	3.04	464	94
B1 - 32	32	32	37	0.74	1.05	1.60	85	2.04	462	94
B1 - 30	13	38	49	0.88	1.15	1.39	91	1.79	555	94
B1 - 28	25	38	38	0.70	1.08	1.70	91	1.29	481	94
B1 - 20	6	20	74	0.89	1.16	1.31	94	1.42	653	94
B1 - 12	30	20	50	0.70	1.01	1.45	87	0.96	503	93

to the PI_{pd} and Tmax values. Generally, vitrinite reflectance values are characterized by a wide range of variation between 0.62% and 1.97%, which decreases gradually with depth. Most of the vitrinite reflectance data presented on the histograms show bi- and multi-modal characteristics.

TRHI generally show higher rank values in the range between 77% and 94% and increase gradually with depth (Table 2).

Volumes of generated methane fluctuate between 77% and 94% and decrease towards the bottom of the member (Table 2).

Discussion

Organic matter content. — One of the most important factors influencing organic matter content in sediment is the biological productivity concentrated in nutrient-rich surficial waters. According to some researchers, the phenomenon should be considered as a key process for accumulation of organic-rich sediments and its appropriate combination with sea currents responsible for distribution and reworking of organic matter and its transportation between production and deposition zones, should guarantee a formation of lithological horizons with high TOC (Canfield 1994; Cowie *et al.* 1995; Holmer 1999).

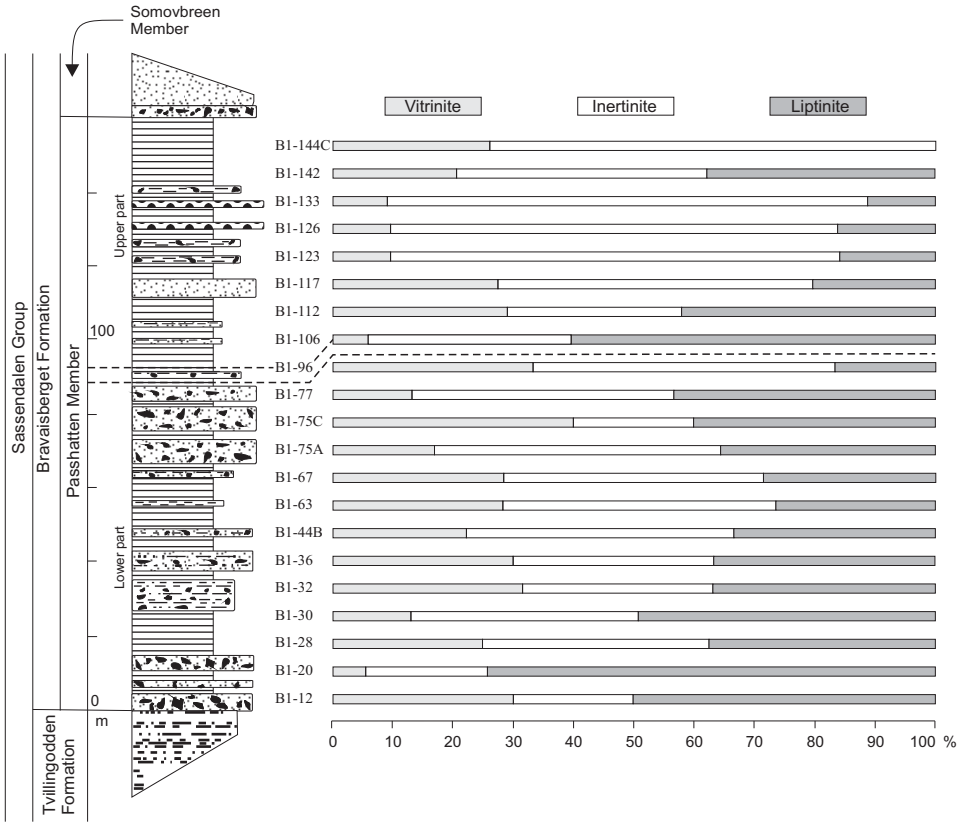

Fig. 4. Simplified section of the Passhatten Mb against the plots of the visible kerogen percentages.

Another important factor influencing organic carbon content in sediment is the oxygenation of bottom waters. However, many authors, especially those who based their research on modern sedimentary environments, suggest that oxygenation does not affect the burial of organic matter (Canfield 1994; Cowie *et al.* 1995; Holmer 1999). However, in contrast, Hulthe *et al.* (1998) considered that the content of buried organic matter may be under the control of oxygenation in the sedimentary environment. Berner and Raiswell (1984) and Hulthe *et al.* (1998) proved that decomposition of organic matter in oxic environments is under the control of: (i) overall resistance of organic matter, (ii) its chemical composition, and (iii) its reactivity. Fresh organic matter decomposes at more or less same rate in anoxic and oxic environments, whilst old and re-deposited organic matter decomposes more quickly in oxic environments. The difference is because degraded organic matter consists of organic macromolecules that are devoid of active functional groups. Anoxic microbes are not able to decompose the organic matter, whereas oxic microbes could decompose the organic matter type (Kristensen *et al.* 1995; Hulthe *et al.* 1998). Oxic and anoxic rates of decomposition are similar only for

freshly settled organic matter in surficial parts of the sedimentary column, because the type of organic matter is characterized by weaker bonds between organic molecules. Fresh organic matter is not usually adsorbed to the surface of mineral grains, but with time, burial and degradation, organic matter adsorbs to the surface of mineral grains and anoxic microbes become less effective. The limited ability of anoxic microbes for decomposing weathered, resistant, and structurally complex organic matter, causes oxic decomposition to be faster and more efficient (Kristensen *et al.* 1995; Hulthe *et al.* 1998).

Other factors that may affect organic matter content are those linked directly with reworking of sediments, such as burrowing and rate of sedimentation. In particular, the latter process has a strong impact on organic matter preservation in shallow shelf sediments, and its richness in hydrogen (Arthur *et al.* 1998).

Microbial degradation of bottom settled or buried organic matter linked with redoxcline fluctuations should also be added to the most destructive factors responsible for reducing organic carbon content (Krajewski 1989; Pedersen *et al.* 1992; Prahl *et al.* 1994; Kristensen *et al.* 1995; Hulthe *et al.* 1998). The process results from a combination of both oxic and anoxic decomposition, which occurs during the transformation of an environment from oxic to anoxic (or *vice versa*). The fusion causes settled organic matter to decompose as a result of the activity of oxic and anoxic microbes (Kristensen *et al.* 1995; Hulthe *et al.* 1998).

Other factors strongly affecting the organic matter content in sediments are organic matter type (Martin and Bender 1988; Berger *et al.* 1989; Prahl *et al.* 1994) and its exposure time at sea bottom (Middelburg 1989).

The relative importance and nature of all these factors varies depending upon the organic matter type. The scale of the degradation is hard to evaluate for each process, but their total influence is more or less predictable. Usually, the degradation processes occur simultaneously with different combinations and therefore, deciphering which one was the most destructive is difficult to estimate. Prediction of TOC_o is important as the difference between TOC_o and TOC_{pd} could help to comprehend the hydrocarbon potential of organic matter and to recognize organic matter type in terms of primary hydrogen-oxygen characteristics (H-O). The maturity path usually only shows the present-day H-O characteristics, and cannot reflect the primary PP of organic matter.

The TOC_{pd} fluctuates in a wide range along the whole section of the Passhatten Mb (Fig. 3) and the variation follows lithological changes. A wide variation in TOC_{pd} values can be found in those lithological horizons dominated by recurrent occurrences of: (i) shales and sandstones, or (ii) different lithological types of black shales, differently bioturbated and enriched in organic matter. The wide range in TOC_{pd} variation is accompanied by wide and regular fluctuations in: (i) the DOP (Degree of Pyritization) in a range between 0.29 and 0.92, and (ii) the $\delta^{34}S$ (sulfur isotopic composition) in a range between -26 and +8‰ VCDT. Correlation between parameters, such as DOP and $\delta^{34}S$ with TOC (Karcz 2009),

and HI to $\delta^{34}S$ (Karcz 2010) suggests hydrogen-depleted organic matter in certain horizons and generally lower average HI_{pd} values (Fig. 5), confirm indirectly the causes of wide TOC_{pd} variation. On the other hand, a narrow range of TOC_{pd} values is coupled with rather petrographically monotonous horizons dominated by black shales only, *e.g.*, B1-28–43, B1-36–44B, B1-45–48, B1-75A–79, B1-96–98, B1-115A– 115C, and B1-121–144B.

Generally, TOC_{pd} values differ slightly between the lower and upper sections of the Passhatten Mb, respectively (B1-12–104 and B1-106–146). The latter section is dominated by somewhat higher TOC_{pd}, averaging ~2.5%, whereas the average TOC_{pd} value in the lower section is ~2.0%. The difference in organic matter content may be due to the predominance of black shales in the upper section, and decreased: (i) bottom current activity, (ii) oxygenation of bottom environment, (iii) amount of bioturbation, and (iv) clastic sedimentation rate. All these causes contributed to a greater share of shale above the sandstone, and correlate well with an increase in stagnation of the bottom environment. Transformation of the environment to one more stagnant is also confirmed by the decreasing input of vitrinite and liptinite macerals towards the top of the Passhatten Mb (Fig. 4), which may suggest some difficulty in the free flow of organic particles from the source areas. In other words, it is probable that the distance between the organics source area and deposition zone has increased.

The presented TOC_o follows the trend of TOC_{pd}. The correlation between these two factors is good and is presents a more or less parallel trend (Fig. 3). The calculated TOC_o values are consistent for sediments deposited under a high biological productivity zone, and also are comparable to the TOC_{pd} values from the eastern Svalbard Botneheia Fm for localities characterized by immature and early mature organic matter (TOC_{pd}: 1–10%; Dallmann *et al.* 1999). The difference between the TOC_o and TOC_{pd} for the Passhatten Mb is almost equal for nearly the whole section of the member. This may suggest that expulsion was almost the same for the whole section, and/or the organic matter consists almost entirely of one organic matter type or a constant mixture.

A negative correlation between the organic matter content and detrital fraction size may not be universal, but occurs relatively frequently, especially on shallow shelves where any changes in dynamics can easily modify detrital fraction size (Ganeshram *et al.* 1999). The latter work considered that a transgression pulse might be responsible for the decrease of the dynamics of the bottom shelf waters. In turn, this might cause a decrease of the detrital fraction size, because of an increase in the distance between the clastics source and accumulation zones. Consequently, the process contributes to minor dilution of organic matter in the sediment and provokes an increase of the total organic matter content in a certain unit volume. A transgression pulse on the shelf may also be responsible for an increase of both biological productivity and organic matter supply to the sea bottom (Dypvik 1985; Ganeshram *et al.* 1999). The relationship between transgression and biological productivity is espe-

cially well coupled on shelves dominated regionally by upwelling currents (Gardner *et al.* 1997; Dean and Gardner 1998). The discussed relationship has also been observed in other sedimentary environments, *e.g.*, the upper Triassic and Jurassic Wilhelmøya and Janusfjellet formations on Spitsbergen (Krajewski 1989). Additionally, the type of organic-rich, fine-grained sediment is characterized by definitely higher PP values (Weisner *et al.* 1990; Pedersen *et al.* 1992).

It is probable that a transgressive pulse of late Anisian (Mørk *et al.* 1989) traceable in a short section of the member between sampling points B1-104 and B1-106, might have caused bottom stagnation and accumulation of organic-rich, fine-grained sediments of the upper Passhatten section. Consequently, the Passhatten Mb consists of two sections: coarser and finer grained with lower and upper TOC and PP values, respectively. These two sections are also accompanied by a lesser and greater share of black shales. The subdivision also reflects poorer and better conditions for organic matter preservation.

Type of organic matter. — According to the van Krevelen diagram, HI_{pd} values positioned in the range between 50 and 125 (mgHC/gTOC) suggest that organic matter in the Passhatten Mb is kerogen II in the upper intermediate stage of thermo-catalytic alteration. The present day H-O characteristic of the kerogen, positioned the sample points close to the boundary between the late katagenetic and early metagenetic zones (Fig. 5). The H-O features also show oxygen-enriched and hydrogen-depleted kerogen II, as a probable result of synsedimentary reworking of organic matter by dysoxic and/or even oxic bottom currents. Consequently, the latter samples should be interpreted as representative of oxygenated marine organic matter residuum, or a certain admixture of land-derived organic matter. An analogous idea was also given by Dean *et al.* (1994) and Dean and Gardner (1998). However, other authors suggest that low HI values cannot be only a result of the domination of land-derived organic matter (Jasper and Gagosian 1990; Ganeshram *et al.* 1999). On the other hand, higher HI values were observed in the planar-laminated lithological horizons of the Passhatten Mb, deposited under dysoxic and/or anoxic conditions. The alteration of H-O characteristics, *i.e.*, the decrease of OI and increase of HI_{pd} values, correlates well with an open marine facies progradation, which occurred during the late Anisian transgression (Mørk *et al.* 1982; Steel and Worsley 1984).

In contrast to the HI_{pd} values trend (upwards increase) is the HI_o values trend, which decreases upwards towards the top of the Passhatten Mb (Fig. 6). The maximum difference between HI_{pd} and HI_o occurs in the lower part of the member and it decreases gradually towards the top of the Passhatten Mb. The highest discrepancy between these parameters is in the lower part of the member, which suggests that the organic matter was fresher and more reactive than the organic matter in the overlaying part of the member. The discrepancy between HI_{pd} and HI_o is a result of: (i) higher organic matter degradation resulting from recurrent occurrences of oxic and anoxic microbial communities, and/or (ii) a higher capacity to expel hy-

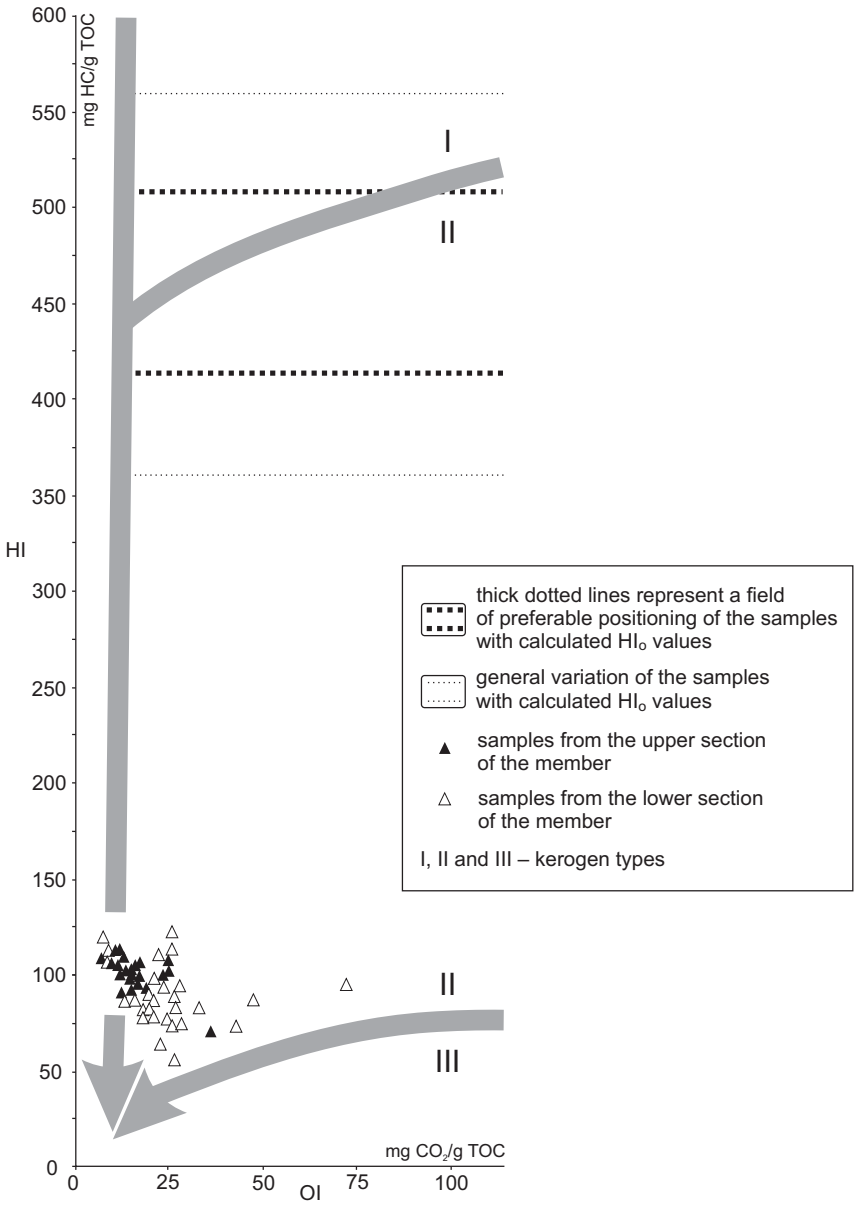

Fig. 5. Hydrogen Index *vs.* Oxygen Index diagram showing difference between two sets of HI values; the initial (calculated) and present day (measured) for samples from the Passhatten Mb.

drocarbons. This also means that the highly fresh and reactive organic matter is mostly marine and autochthonous in origin. The S1/TOC ratio based on the scheme of Hunt (1996) confirms the correctness of the idea (Fig. 7A). Consequently, the autochthonous organic matter should be considered as having been deposited under a productive zone.

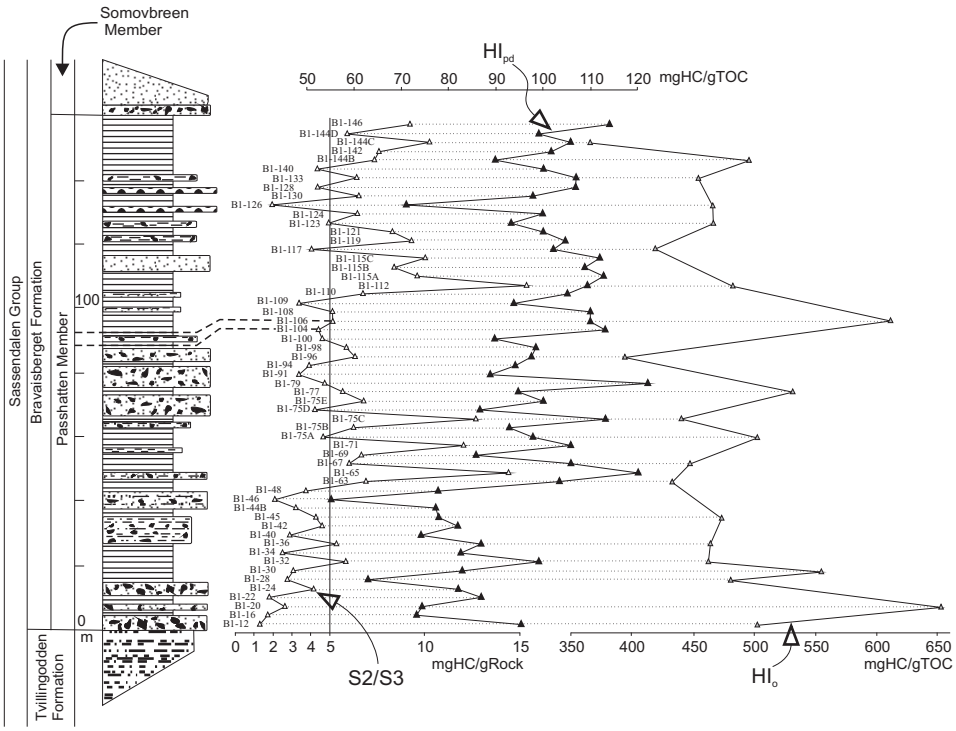

Fig. 6. Negative correlation between HI_{pd} and HI_o suggests some differences in organic matter reactivity, decomposition, and expulsion efficiency for hydrocarbons.

In contrast to the large discrepancy between HI_{pd} and HI_o, are the data from the upper part of the member where the difference is much smaller, indicating favorable conditions for organic matter preservation, and/or smaller hydrocarbon expulsion caused by a smaller transformation coefficient. The idea correlates well with data concerning a shift in the high biological productivity zone after the late Anisian transgression (Karcz 2010). Consequently, the upper part of the member has not been deposited under a high biological productivity zone, but in its proximity. As shown by the HI_o calculations and the range of preferable and subordinary positioning of the sampling points after adjustment for the hydrogen loss, the primary source of organic matter was oil-prone organic matter, similar to kerogen I and II types, *i.e.*, hydrogen-rich marine organic matter (phytoplankton) with a subordinate admixture of also hydrogen-rich, land-derived organic matter (Fig. 5).

Ganeshram *et al.* (1999) showed reasons for high TOC and HI values. They suggested that sediments with high HI and TOC values can be deposited under both oxic and anoxic conditions, and are independent from oxygenation. In contrast to this idea are Passhatten's data, which show an increase in HI and TOC values towards the top of the member (Fig. 7F). The geochemical data correlate

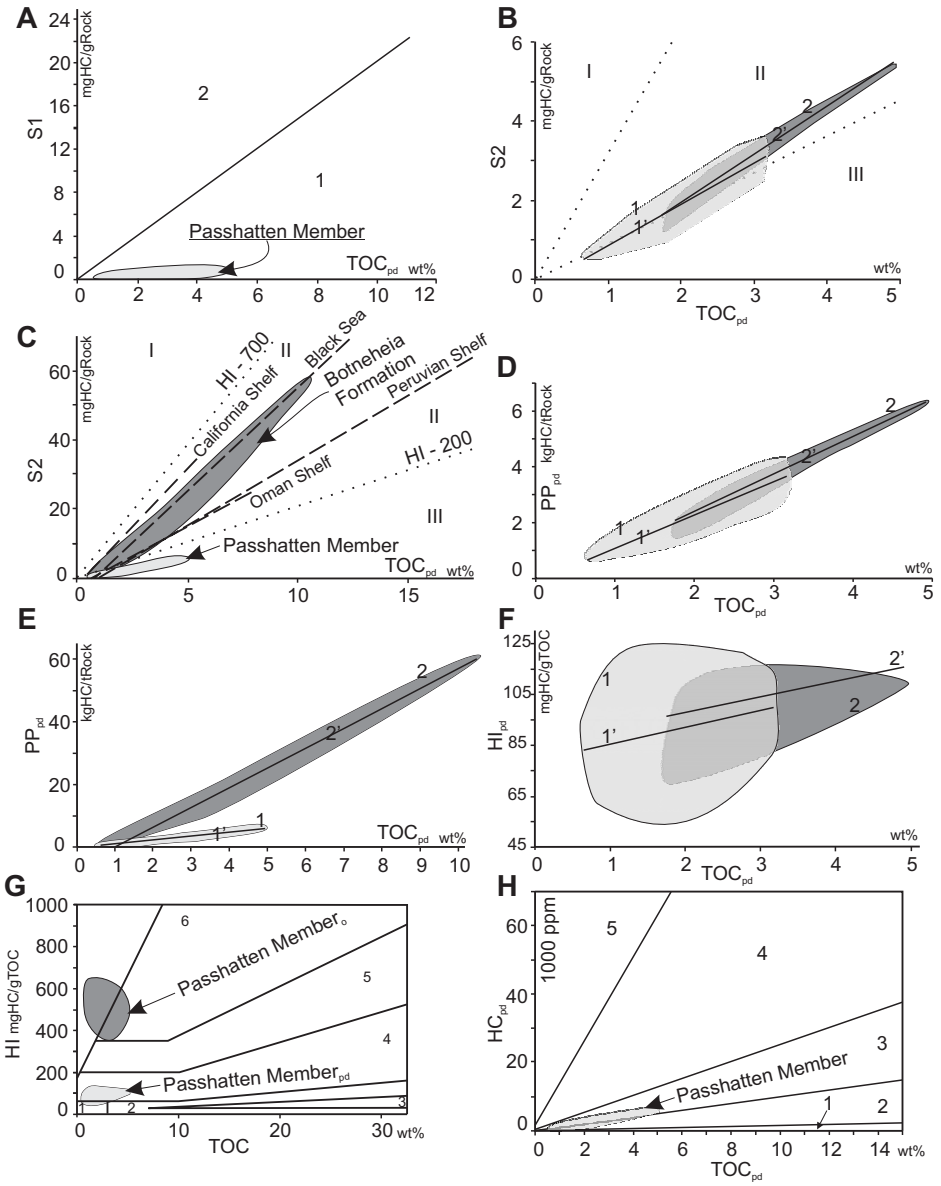

Fig. 7. Correlations-sheet from samples of the Passhatten Mb. A: 1 and 2: fields of autochthonous and allochthonous organic matter, respectively (after Hunt 1996). B, D, F: 1 and 1'; 2 and 2': field of data range and regression line for the lower and the upper part of the Passhatten Mb, respectively. C – Botneheia Fm (Krajewski 2013); Peruvian shelf (Suess *et al.* 1987); Oman shelf (Pedersen *et al.* 1992); Black Sea (Arthur *et al.* 1998); California shelf (Dean and Gardner 1998). E – 1 and 1'; 2 and 2': field of data range and regression line for the Passhatten Mb and the Botneheia Fm, respectively, data for Botneheia Fm (Krajewski 2013). G: 1 – field of poor source of oil; 2 – oil and gas field; 3 – gas field; 4 – medium source of oil; 5 – good source of oil; 6 – very good source of oil; (after Jackson *et al.* 1985). H: 1 – poor PP field; 2 – some gas potential field; 3 – gas field with some potential of oil; 4 – oil and gas field; 5 – HC migration field; (after Sari and Aliyev 2006).

well with sedimentological and petrographical features reflecting the total absence of oxygen, or at least its deficiency in the environment, *e.g.*, a number of parallel–laminated solid black shale lithological horizons, enriched in euhedral crystals of pyrite, increase towards the top of the member. Therefore, both HI and TOC parameters are dependent on oxygenation, and both control the hydrocarbon potential.

The domination of marine organic matter is also confirmed by the S2/TOC ratio according to the classification proposed by Langford and Blanc-Valleron (1990) (Fig. 7B). According to the suggestions of Dean and Gardner (1998), the degree of positive shift of the regression line results from some share of land-derived organic matter, and positive correlation is the result of a high volume of reactive organic matter. A positive shift of the regression line can also be the result of organic matter adsorption on the surface of mineral grains (Katz 1984; Ganeshram *et al.* 1999) or limitation in the detection of hydrocarbons during the pyrolysis process (Langford and Blanc-Valleron 1990). The positive correlation for the data of the Passhatten Mb shows the domination of reactive, fresh marine organic matter, but a shift of the regression line also shows that some share of residual and/or land-derived organic matter is highly reliable. The S2/S3 relationship based on the scheme of Clementz *et al.* (1979) confirms the idea (Fig. 6).

The correlation data of the Passhatten Mb and the Botneheia Fm, which is age-equivalent from a deeper shelf in eastern Svalbard, shows the difference in maturity between these lithostratigraphic units (Fig. 7C). The latter figure shows that the organic matter of the Passhatten Mb is kerogen III. The interpretation is a result of maturity/over-maturity of organic matter in the Passhatten Mb, and changed organic carbon *versus* hydrocarbon ratio because of hydrocarbon expulsion. In contrast to the Passhatten's data, the Botneheia Fm is dominated by type II kerogen, which carries S2-TOC characteristics similar to the Black Sea organic-rich sediments deposited in the Holocene (Arthur *et al.* 1998). The primary goal of that correlation was to understand the bio-geo-chemical conditions of the bottom environment. Therefore, it seems to be reliable that the bottom environment during the accumulation of the Passhatten Mb was euxinic or semi-euxinic. In other contemporary marine environments, plankton-derived kerogen dominates with a small admixture of land-derived organic matter (Bergamaschi *et al.* 1997; Arthur *et al.* 1998). In these environments, especially those under the control of upwelling currents, a positive shift of the TOC *versus* S2 values usually occurs. Examples of these environments are the Oman and Peruvian shelves (Suess *et al.* 1987; Pedersen *et al.* 1992). The Botneheia Fm at the presented Blanknuten location is early mature and mature in respect of oil generation, but has not expelled hydrocarbons (Schou *et al.* 1984; Krajewski 2000d) and thus, the data represent approximate initial organic carbon content. This indicates that the Passhatten Mb was deposited in dynamic conditions of a shallow shelf where bio-geo-chemical conditions were strongly reducing at the bottom zone.

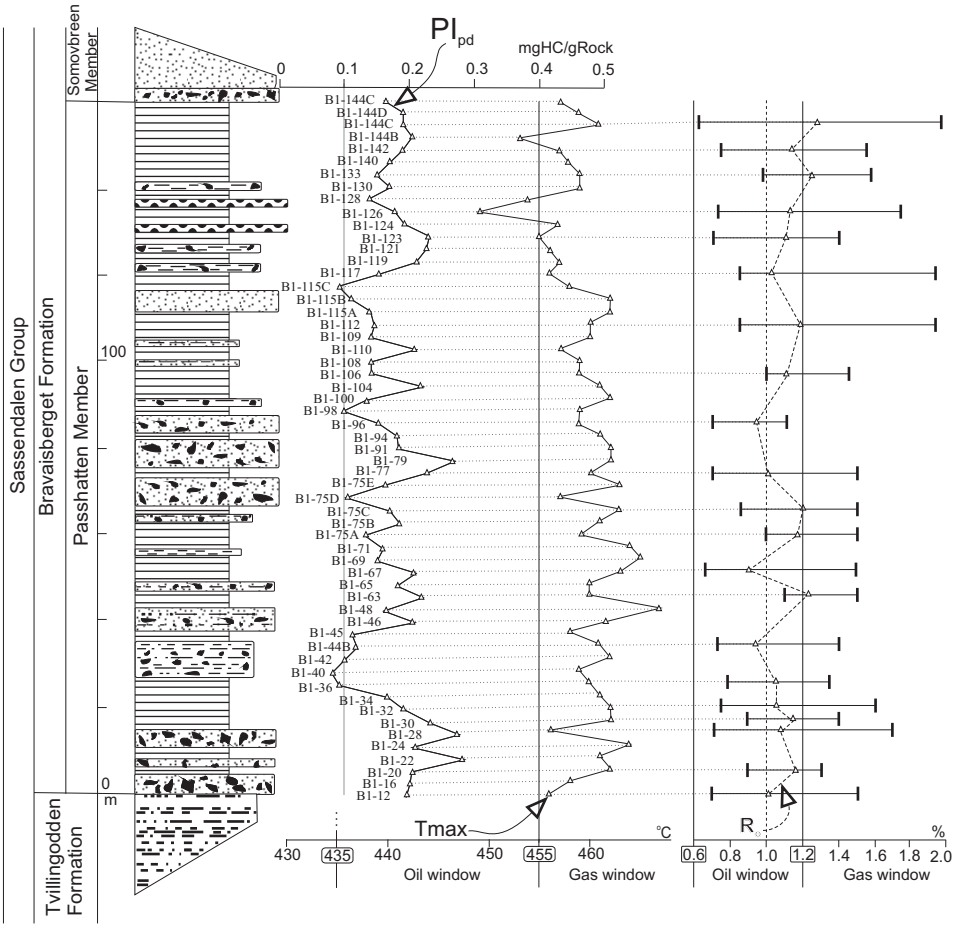

Fig. 8. The plot of the maturity indicators shows significant discrepancy between the range of maturity suggested by Tmax and R_o data, which may be a result of vitrinite impregnation by bitumen.

Organic matter maturity. — The predomination of Tmax values above 455°C suggests that the organic matter in the Passhatten Mb, at the section of Bravaisberget, is overmature for petroleum generation. These values are inconsistent with the PI_{pd} and vitrinite reflectance suggesting that the member contains early-mature to mature organic matter for petroleum generation (Fig. 8). The TRHI, RC_{pd}-TOC_{pd} and calculated volume of generated methane fluctuate between 85% and 95%, which also point to an upper part of gas window (Fig. 9). Then, the inconsistency between the vitrinite reflectance and other parameters may be explained by the probable bitumen appearance decreasing vitrinite reflectance values downwards. The presence of residual bitumen or retained oil in the host rock can influence reflectance when the bitumen impregnates the vitrinite (Robert 1988) and oil fills the pores and/or pore throats. On the other hand, TRHI,

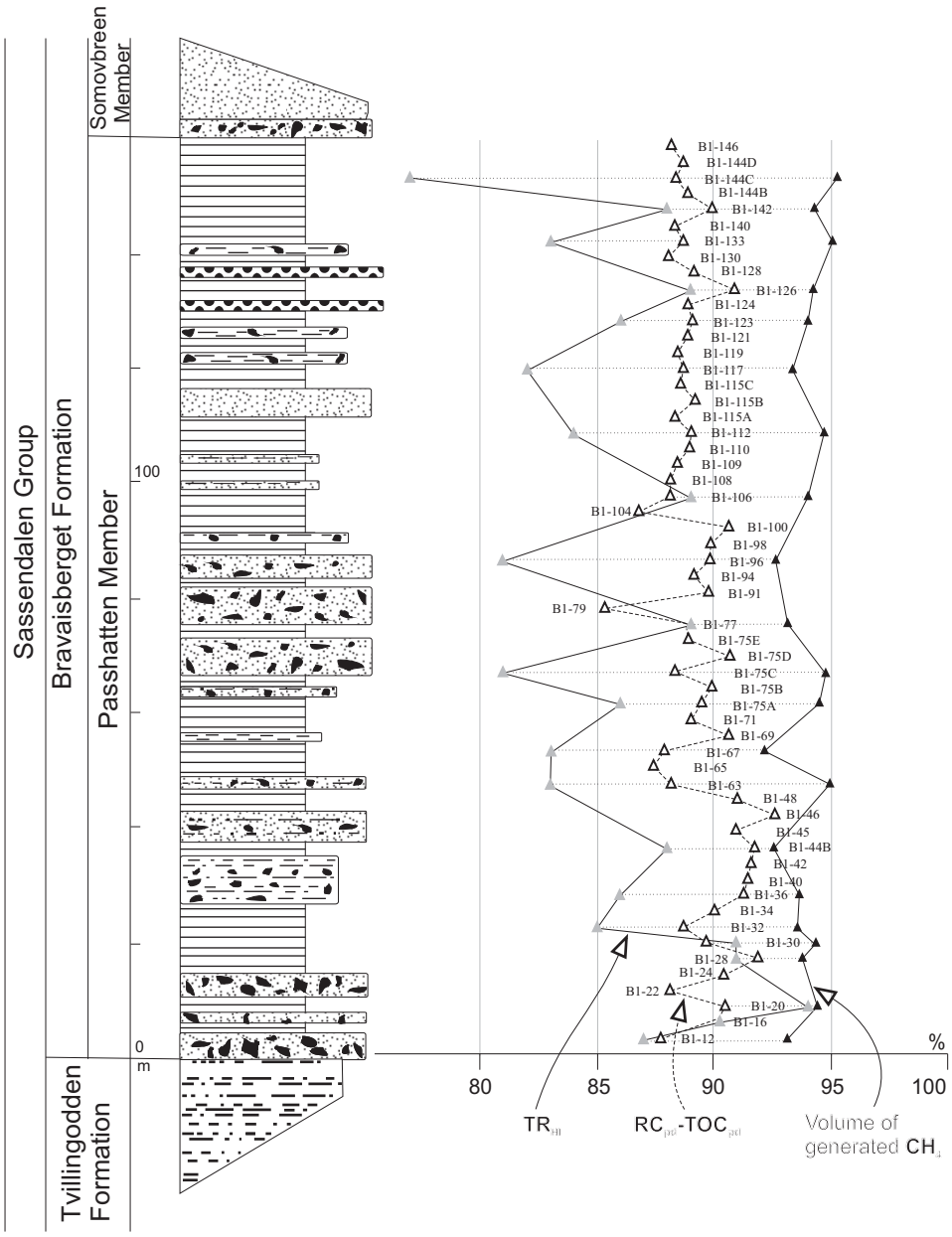

Fig. 9. The plot of supplemental maturity indicators shows increase of maturity with decrease of volume of generated methane. Probably the key factor controlling this discrepancy is decreasing downwards TOC.

RC_{pd}-TOC_{pd} and Tmax data increasing consistently downwards reflect the typical trend in maturity. Moreover, upper intermediate rank of organic matter coalification is also suggested by domination of multi- and bi-modal reflectance in the

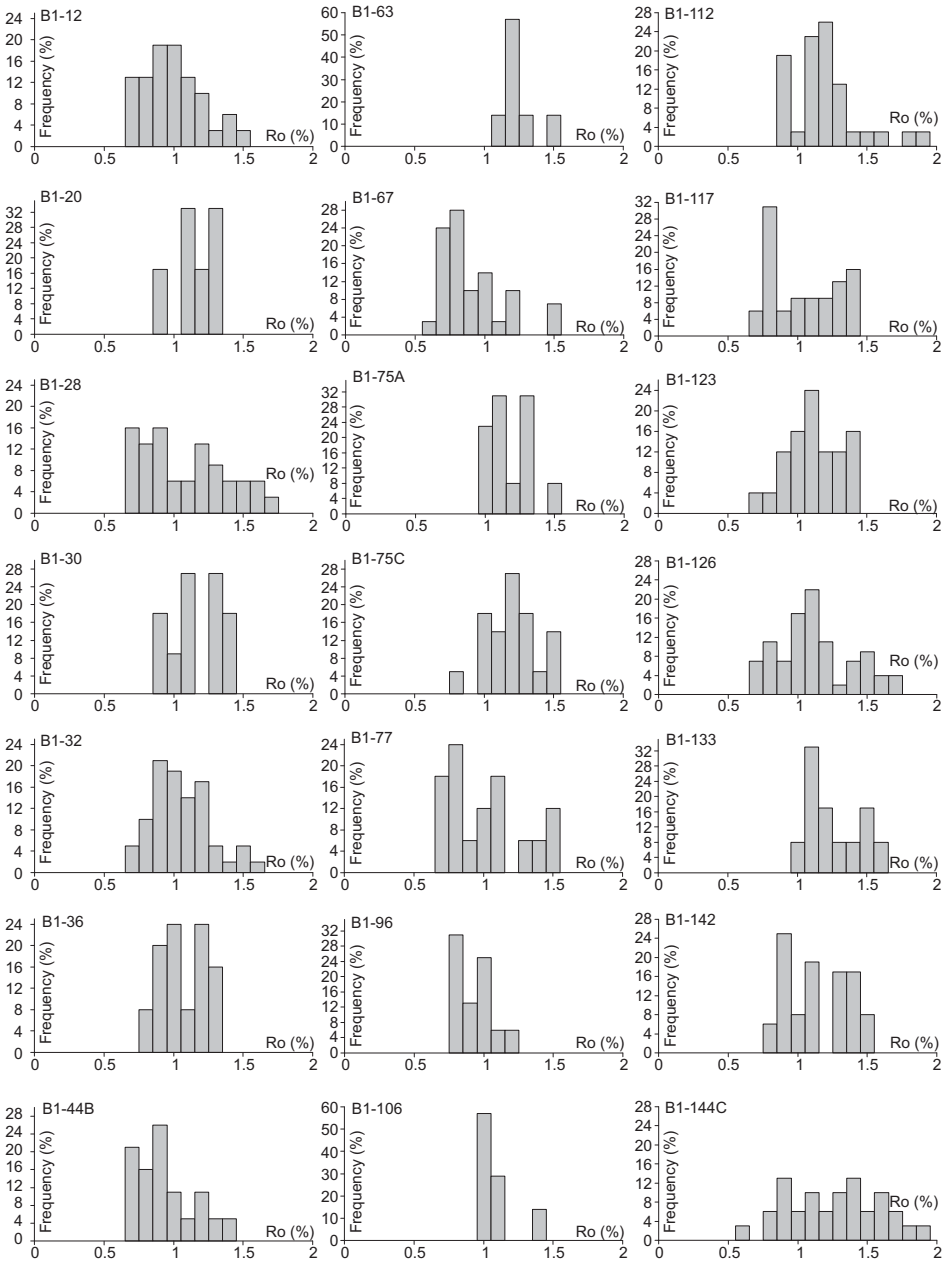

Fig. 10. Histogram sheet showing domination of the bi- and multi-modal histograms for samples from the Passhatten Mb.

histograms (Fig. 10), although these results can be also caused by certain admixtures of land-derived organic matter. Krajewski (2000e) confirmed an occurrence of varying admixture of highly degraded fibrous, woody and coaly debris in the

Treskelen section of the Passhatten Mb. Therefore, an occurrence of land derived organic material is also presumable in the Bravaisberget section. Consequently, the lower reflectance in multi- and bi-modal histograms may reflect autochthonous material and the appropriate degree of organic metamorphism, whilst higher values of reflectance are linked with a reworked terrestrial fraction.

Petroleum potential of the Passhatten Mb. — According to classification of Bordenave (1993) and Sari and Aliyev (2006), almost 70% of the samples are in the range of middle PP_{pd} values from 2 to 6 (kgHC/tRock). 30% of the samples are in the range of the gas generation zone (<2 kgHC/tRock) and only one sample (B1-112) is in the range of good PP_{pd} (>6 kgHC/tRock; Fig. 11).

PP_{pd} values for the Passhatten Mb and the Botneheia Fm, show that the initial genetic potential of the Passhatten Mb might have been considerably higher. The difference in PP_{pd} values between these two lithostratigraphic units may only reflect the initial evaluation of the expelled HC migrated out of the Passhatten rock unit. PP_{pd} of the Botneheia Fm reaches up to 60, average 21 (kgHC/tRock;

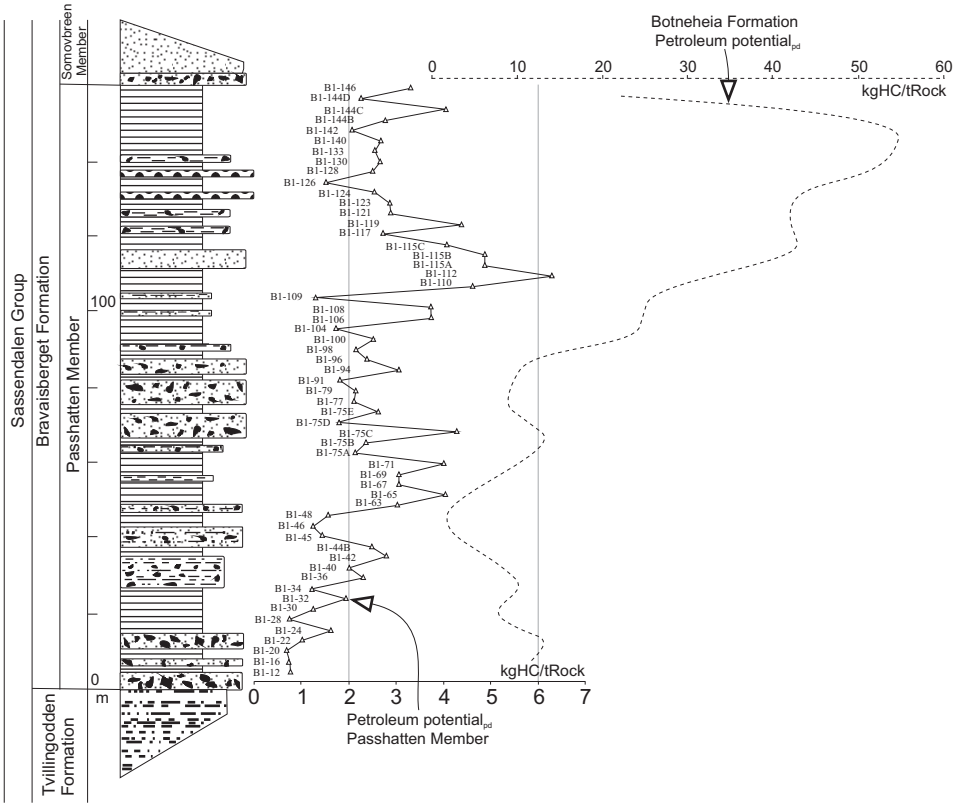

Fig. 11. The comparison of the petroleum potentials from much and less matured locations of Svalbard, *i.e.*: the Passhatten Mb (western Svalbard-Bravaisberget Block) and the Botneheia Fm (eastern Svalbard-Blanknuten; Krajewski 2013).

Krajewski 2013). On the other hand, the lower PP_{pd} in the Passhatten Mb suggests that the member has gone through the oil and is presently in the gas window.

Positive correlation values between PP_{pd} and TOC_{pd} suggest that organic carbon content is the key factor for formation of the PP parameter (Fig. 7D). In highly matured sediments, the PP_{pd} increase is not too great, especially in units near the oil-gas window transition, or entirely enclosed in the gas window, as with the Passhatten Mb (Fig. 7E).

The relationship between HI and TOC can also be useful for PP interpretation (Hunt 1996; Sari and Aliyev 2006). Positive HI-TOC correlation usually occurs in planar-laminated organic carbon- and hydrogen-rich sediments (>1% – TOC and >60 mgHC/gTOC – HI; Ganeshram *et al.* 1999; Sari and Aliyev 2006). While, a negative correlation is usually caused by: (i) constant HI values as an effect of a single source of organic matter (Langford and Blanc-Valleron 1990), and (ii) low organic carbon content (Erik *et al.* 2006). The Passhatten Mb's present day and initial data vary relative to each other. Present day data show a positive correlation, whereas initial data demonstrate a negative correlation. The maturation path from initial to present day data reveals excellent PP_o, which with burial of the member and Cenozoic tectogenesis, have been almost entirely completed (Fig. 7G). Moreover, the HC-TOC relationship displays good potential for gas generation (Fig. 7H).

In order to present any PP in real numbers, the PP has been evaluated to an artificially established unit of the Bravaisberget Block. Calculation of generated hydrocarbons from the Passhatten Mb black shales in the Bravaisberget Block has been conducted according to the assumption of general low lateral data variation within the block (Bjorøy *et al.* 1980; Mørk *et al.* 1989; Dallmann 1999; Egorov and Mørk 2000; Krajewski 2000a; Krajewski *et al.* 2007). This assumption includes the black shales thickness, density, and petrological and geochemical data. The vertical changes caused by the transgressive pulse of the late Anisian covered the whole Bravaisberget Block area. Consequently, lateral variation of data for the Bravaisberget Block is low for the entire examined section and most lithological horizons within the unit. The block in the Middle Triassic interval was dominated almost entirely by a distal shallow shelf with a subordinate share of proximal shallow shelf facies (Krajewski 2000a). The two facies have been dominated by black shale lithological horizons distributed regularly in both lateral and vertical surfaces. The whole block is located within the West Spitsbergen Fold Belt (WSFB; Fig. 1) and therefore, the black shales are characterized by satisfactory maturity with respect to gas potential considerations. The Bravaisberget Block should only be considered in terms of unit volume attributed to the Passhatten Mb within the boundaries presented in Fig. 1.

The Middle Triassic horizons surrounding the Bravaisberget Block pass gradually into the proximal shallow shelf and delta front environment to the west (Krajewski 2000a), causing a different contribution of black shales with respect to

the member thickness from the presented location. The thickness of the Passhatten Mb also decreases southwards (average 109 m) causing the thickness of the black shales to be reduced to about 48 m in the Treskelen area (Krajewski 2000a; Mørk and Bromley 2008). However, the maturity of the organic matter in the Treskelen location is relatively high, averaging 2.19% R_o (Krajewski 2000e). The Passhatten Mb to the east of the Bravaisberget Block has not been recognized in southern Spitsbergen (eastern Nordenskiöld Land, Heer Land, eastern Nathorst and Torell Lands). The thickness of the Passhatten Mb decreases slightly northwards (average 201 m in the Festingen area) with the black shale thickness increasing to about 106 m (Krajewski 2000a; Mørk and Bromley 2008). Consequently, oil and gas potential for the surrounding areas should be considered independently.

Taking into consideration the dimensions of the Bravaisberget Block (approx. length and width: 9 and 2 km, respectively) and thickness of the black shales in the block (approx. 0.1 km) and other data, such as rock density (approx. 2.59 g/cm^3), the calculated volume of generated hydrocarbons amount to $3.98 \cdot 10^{10}$ kgHC (Table 3). The value recalculated for gas amounts to $3.98 \cdot 10^{12}$ (ft^3) of gas (*i.e.*, $1.13 \cdot 10^{11}$ m^3; Table 3). Using the data from Table 4, necessary for the methodology applied by Jarvie *et al.* (2007), the gas generated amounts to 679 mcf/ac-ft. This value recalculated and applied to the examined unit volume of 1.8 km^3 is $2.80 \cdot 10^{10}$ m^3. Thus, an average volume of generated gas is $7.05 \cdot 10^{10}$ m^3. With regards to the fact that almost 58% (395 mcf/ac-ft) of generated gas has not been expelled from the source rock unit, an unexpelled gas volume ranges between $1.63 \cdot 10^{10}$ and $6.55 \cdot 10^{10}$ m^3, with an average value of $4.09 \cdot 10^{10}$ m^3 (Table 5).

The displayed disagreement results from the different methodologies applied. Considerations concerning the calculations of minimum values according to the

Table 3

Calculation of generated hydrocarbons from samples of the Passhatten Mb in the Bravaisberget Block based on the methodology described by Schmoker (1994). # – data from Krajewski *et al.* (2007); + – data from Krajewski (2000e).

Factor	Volume of unit: only Passhatten shales in the Bravaisberget Block				Black shales density	HC generated	Gas generated		Oil generated
	Lenght	Width	Thickness	Volume					
Unit	[km]	[km]	[km]	[km^3]	[g/cm^3]	[kg HC]	[ft^3]	[m^3]	[bbl]
Average	9	2	0.1#	1.8	2.59+	$3.98\ 10^{10}$	**$3.98\ 10^{12}$**	**$1.13\ 10^{11}$**	**$3.98\ 10^{8}$**

Table 4

Average values of organic petrological and geochemical parameters from samples of the Passhatten Mb.

Factor	Liptinite	Inertinite	Vitrinite	TOC_{pd}	HI_{pd}	RC_{pd}	PI_{pd}
Unit	[%]	[%]	[%]	[wt%]	[mgHC/gTOC]	[%]	[%]
Average	34	44	22	2.21	95	1.97	0.17

Table 5

Average data of generated and unexpelled gas. * – data after correction with regard to the volume of the Bravaisberget Block from Table 3.

	According to methodology of Schmoker 1994	Jarvie et al. 2007	AVG
	[m^3]	[m^3]	[m^3]
Gas generated	**1.13 10^{11}**	**2.80 10^{10} ***	**7.05 10^{10}**
Gas unexpelled	**6.55 10^{10}**	**1.63 10^{10} ***	**4.09 10^{10}**

Table 6

Set of calculated initial TOC and its constituents with an insight to generated HC data. * – legend as in Table 5.

TOC_o					
2.77 wt %					
PC_o					**RC_o**
1.00 wt %					1.78 wt %
Expelled HC		**Unexpelled HC**			
0.60 wt %		0.40 wt %			
Expelled oil	**Expelled gas**	**Carbon in unexpelled gas**	**Carbon in unexpelled oil**	**RC secondary cracking of oil**	**Total RC**
0.42 wt %	0.18 wt %	0.12 wt %	0.13 wt %	0.14 wt %	1.92 wt %
111 bbl oil/ac-ft	284 mcf/ac-ft	395 mcf/ac-ft			
0.014 m^3/m^3	6.53 m^3/m^3	9.06 m^3/m^3			
2.57 10^7 m^3*	1.17 10^7 m^3*	1.63 10^{10} m^3*			

method of Jarvie *et al.* (2007), allows the estimation of minimum PC_o, RC_o, conversion and expulsion data and their internal relationships.

Consequently, the calculated TOC_o (2.77 wt %) values for the Passhatten Mb consist of PC_o (1.00 wt %) and RC_o (1.78 wt %) (Table 6). Expulsion estimated at 60% allows for the evaluation of expelled HC (as a function of organic carbon content) from primary cracking of kerogen at 0.60 wt % of carbon. Of the latter value, 0.42 wt % of carbon was converted to oil (*i.e.* 70%), while 0.18 wt % of carbon was converted to gas. These values recalculated on oil and gas suggest 111 bbl oil/ac-ft and 284 mcf/ac-ft (or $1.17 \cdot 10^7$ m^3 of gas for the whole of the Bravaisberget Block; Table 6). Unexpelled carbon, which was further cracked to gas, was estimated at 0.40 wt %. The latter value includes the carbon in unexpelled gas from the primary cracking of kerogen (0.12 wt %), carbon in unexpelled oil cracked to gas (0.13 wt %), and residual carbon from secondary cracking of oil (0.14 wt %). About 0.25 wt % of carbon is still retained as gas. The value can be recalculated at 395 mcf/ac-ft ($1.63 \cdot 10^{10}$ m^3 for the Bravais-

berget Block; Table 6). The value of 395 mcf/ac-ft of unexpelled gas may be classified as middle value. The ratio between primary and secondary cracking was estimated at 72% and 28%, respectively.

Conclusions

Deposition of the organic-rich black shales of the Passhatten Mb is a consequence of the overwhelming predominance of favorable over destructive conditions for organic matter preservation in the Middle Triassic shallow shelf of Svalbard. The favorable conditions were supported by high biological productivity, a fast supply of organic particles to the bottom setting, a relatively low sedimentation rate, and reducing bottom conditions. The group of destructive conditions included oxygenated reworking bottom currents coupled with redoxcline fluctuations and burrower activity. As a result of the overlap of these processes with varying intensities, the organic carbon content fluctuates widely, reaching the lowest and highest amounts in densely laminated, striped and non-laminated, solid black shale horizons, respectively. The decrease in the detrital fraction size was probably enforced by the late Anisian transgression and increased bottom stagnation, which might have significant impact on the organic carbon content.

The Passhatten Mb is dominated by autochthonous marine organic matter classified as kerogen II. The basic organic contribution is accompanied by some admixture of oxygenated and reworked residuum of marine or land-derived organic matter. The primary source of the organic matter was highly reactive and hydrogen-rich organic matter derived from a biological productivity zone located nearby.

Cenozoic tectonics uplifted and transformed the shales along the western margin of Spitsbergen. Therefore, the Bravaisberget Block is characterized by thermally altered kerogen II in upper intermediate rank of maturation. The initial TOC and HI values (2.77 wt % and 481 mgHC/gTOC, respectively) were reduced to 2.21 wt % and 95 mgHC/gTOC, respectively, by HC generation and expulsion. The transformed organic matter accomplished almost entirely its oil potential from presumably almost 60 kgHC/tRock, to the range of 0.69–6.30 kgHC/tRock. Primary cracking of the kerogen and oil played a major role in gaseous hydrocarbons generation. While, secondary cracking of oil acts only as a minor function in thermogenic gas generation at that stage of maturity. An estimated 60% expulsion efficiency indicates that the remaining 40% of unexpelled gas, evaluated as 395 mcf/ac-ft in the Bravaisberget Block, allows the consideration of the Passhatten Mb as a potential commercial target. Maturation indicators as R_o, Tmax, TRHI, and HI show that the member meets all the minimum conditions of maturity that may suggest economic viability and cost-effective gas flow.

Acknowledgements. — The author would like to thank Professor Krzysztof P. Krajewski from the Institute of Geological Sciences of the Polish Academy of Sciences (IGS-PAS) for his scientific supervision of PhD dissertation presented partly in this paper and for reviewing of this article. The author would like to also thank the IGS-PAS for providing samples necessary to that dissertation and organic petrological studies and Professor Tadeusz Peryt from the Polish Geological Institute-National Research Institute (PGI-NRI) with Dr Mark KeYang Ma from the SRK Consulting for their helpful suggestions after reading the first draft of the manuscript and Professor Atle Mørk from the SINTEF for reviewing of this article. Dr Izabella Grotek from the PGI-NRI is greatly acknowledged for teaching me to use microscope designed to study organic matter, checking vitrinite reflectance measurements with maceral contents and helpful discussions regarding the all organic petrological data presented in this paper. I am also grateful to Professor Irena Matyasik from the Oil and Gas Institute for Rock Eval analysis. The study was financially supported by the IGS-PAS through statutory and scientific grants of the State Committee for Scientific Research (Research Project No. 6PO4D04120) and the Ministry of Science and Higher Education (Research Project No. PBZ-KBN-108/PO4/2004). Organic petrological data were financially supported by the PGI-NRI through statutory grant (Research Project No. 61.5105.0801.00.0).

References

ARTHUR M.A., DEAN W.E. and LAARKAMP K. 1998. Organic carbon accumulation and preservation in surface sediments on the Peru margin. *Chemical Geology* 152: 273–286.

BERGAMASCHI B.A., TSAMAKIS E., KEIL R.G., EGLINTON T.I., MONTLUCON D.B. and HEDGES T.I. 1997. The effect of grain size and surface area of organic matter, lignin and carbohydrate and molecular compositions in Peru margin sediments. *Geochimica et Cosmochimica Acta* 61: 1247–1260.

BERGER W.H., SMETACEK V.S. and WEFER G. 1989. *Productivity of the oceans. Present and past*. Wiley and Sons, New York: 471 pp.

BERNER R.A. and RAISWELL R. 1984. C/S method for distinguishing freshwater from marine sedimentary rocks. *Geology* 12: 365–368.

BIRKENMAJER K. 1977. Triassic sedimentary formations of the Hornsund area, Spitsbergen. *Studia Geologica Polonica* 51: 7–74.

BJORØY M., MØRK A. and VIGRAN J.O. 1980. Organic geochemistry of Triassic rocks from Bjørnøya. Institute for Kontinental Sokkelundersøkelser, Open Report 160/2/80.

BORDENAVE M.L. 1993. Applied petroleum geochemistry. *In*: M.L. Bordenave (ed.) *Exploration Division*.Total, Paris: 561 pp.

BURNHAM A.K. 1989. On the validity of the pristine formation index. *Geochimica et Cosmochimica Acta* 53: 1693–1697.

CANFIELD D.E. 1994. Factors influencing organic carbon preservation in marine sediments. *Chemical Geology* 114: 315–329.

CLEMENTZ D.M., DEMAISON G.J. and DALY A.R. 1979. Well site geochemistry by programmed pyrolysis. *Proceedings, Eleventh Annual Offshore Technology Conference* 1: 465–470.

COWIE G.L., HEDGES J.I., PRAHL F.G. and LANGE G.J. 1995. Elemental and major biochemical changes across an oxidation front in a relict turbidite: An oxygen effect. *Geochimica et Cosmochimica Acta* 59: 33–46.

DALLMANN W.K. 1999. *Lithostratigraphic lexicon of Svalbard. Upper Paleozoic to Quaternary Bedrock. Review and Recommendations for Nomenclature Use*. Norsk Polarinstitutt, Tromsø: 318 pp.

DEAN W.E. and GARDNER J.W. 1998. Pleistocene to Holocene contrasts in organic matter production and preservation on the California continental margin. *Geological Society of America Bulletin* 110: 888–899.

DEAN W.E., GARDNER J.W. and ANDERSON R.Y. 1994. Geochemical evidence for enhanced preservation of organic matter in the oxygen minimum zone of the continental margin of northern California during the late Pleistocene. *Paleoceanography* 9: 47–61.

DYPVIK H. 1985. Jurassic and Cretaceous black shale of the Janusfjellet Formation, Svalbard, Norway. *In*: R. Hesse (ed.) Sedimentology of Siltstone and Mudstone. *Sedimentary Geology* 41: 235–248.

EGOROV A.Y. and MØRK A. 2000. The East Siberian and Svalbard Triassic successions and their sequence stratigraphical relationships. *Zentralblatt für Geologie und Paläontologie I*: 1377–1430.

ERIK N.Y., ÖZCELIK O. and ALTUNSOY M. 2006. Interpreting Rock-Eval pyrolysis data using graphs of S2 vs. TOC. Middle Triassic–Lower Jurassic units, eastern part of SE Turkey. *Journal of Petroleum Science and Engineering* 53: 34–46.

ESPITALIÉ J., LA PORTE J.L., MADEC M., MARQUIS F., LE PLAT P., PAULET J. and BOUTEFEU A. 1977a. Méthode rapide de caractérization des roches méres de leur potential pétrolier et de leur degreé d'évolution. *Reveu de l'Institute Francais du Pétrole* 32: 23–42.

ESPITALIÉ J., MADEC J.M., TISSOT B., MENNING J.J. and LE PLAT P. 1977b. Source rock characterization method for petroleum exploration. *Proceedings 1977, Offshore Technology Conference* 3: 23–42.

GANESHRAM R.S., CALVERT S.E., PEDERSEN T.F. and COWIE G.L. 1999. Factors controlling the burial of organic carbon in laminated and bioturbated sediments off NW Mexico: Implications for hydrocarbon preservation. *Geochimica et Cosmochimica Acta* 63: 1723–1734.

GARDNER J.V., DEAN W.E. and DARTNELL P. 1997. Biogenic sedimentation beneath the California current system for the past 30 k.y. and its paleoceanographic significance. *Paleoceanography* 12: 207–225.

HOLMER M. 1999. The effect of oxygen depletion on anaerobic organic matter degradation in marine sediments. *Estuarine, Coastal and Shelf Science* 48: 383–390.

HULTHE G., HULTH S. and HALL P.O.J. 1998. Effect of oxygen on degradation rate of refractory and labile organic matter in continental margin sediments. *Geochimica et Cosmochimica Acta* 62: 1319–1328.

HUNT J.M. 1996. *Petroleum Geochemistry and Geology*. W.H. Freeman and Company, New York: 743 pp.

INTERNATIONAl COMMITTEE FOR COAL PETROLOGY (ICCP). 1998. The New Vitrinite Classification (ICCP System 1994). *Fuel* 77: 349–358.

JACKSON K.S., HAWKINS P.J. and BENNETT A.J.R. 1985. Regional facies and geochemical, evaluation of southern Denision Trough. *Australian Petroleum and Exploration Association Journal* 20: 143–158.

JARVIE D.M., HILL R.J., RUBLE T.E. and POLLASTRO R.M. 2007. Unconventional shale-gas systems: the Mississippian Barnet Shale of north-central Texas as one model for thermogenic shale-gas assessment. *American Association Petroleum Geologists Bulletin* 91: 475–499.

JASPER J.P. and GAGOSIAN R.B. 1990. The sources and deposition of organic matter in Late Quaternary Pigmy Basin, Gulf of Mexico. *Geochimica et Cosmochimica Acta* 54: 1117–1132.

KARCZ P. 2008. *Geneza czarnych facji triasu środkowego na Spitsbergenie na podstawie wskaźników geochemicznych*. Dysertacja doktorska, Instytut Nauk Geologicznych Polskiej Akademii Nauk, Warszawa: 161 pp. (in Polish).

KARCZ P. 2009. *Badania z zakresu petrologii organiki – zależności pomiędzy dominującymi typami macerałów, ich zawartością, stopniem dojrzałości a rozwojem horyzontów roponośnych na podstawie wybranych obszarów badań (wysoce produktywny trias zachodniego Spitsbergenu vs.*

trias Wału Kujawskiego). Projekt statutowy Państwowego Instytutu Geologicznego-Państwowego Instytutu Badawczego, Warszawa: 35 pp. (in Polish).

KARCZ P. 2010. Relationships between development of organic-rich shallow shelf facies and variation in isotopic composition of pyrite (Middle Triassic, Spitsbergen). *Polish Polar Research* 31: 239–254.

KATZ B.J. 1984. Source quality and richness of the Deep Sea Drilling Project site 535 sediments, southeastern Gulf of Mexico. *In*: R.I. Buffler *et al.* (eds) *Initial Reports of the Deep Sea Drilling Project* 77: 445–450.

KRAJEWSKI K.P. 1989. Organic geochemistry of a phosphorite to black shale transgressive succession: Wilhelmøya and Janusfjellet Formations (Rhaetian–Jurassic) in Central Spitsbergen, Arctic Ocean. *Chemical Geology* 74: 249–263.

KRAJEWSKI K.P. 2000a. Phosphogenic facies and processes in the Triassic of Svalbard. *Studia Geologica Polonica* 116: 7–84.

KRAJEWSKI K.P. 2000b. Isotopic composition of apatite-bound sulphur in the Triassic phosphogenic facies of Svalbard. *Studia Geologica Polonica* 116: 85–109.

KRAJEWSKI K.P. 2000c. Diagenetic recrystallization and neoformation of apatite in the Triassic phosphogenic facies of Svalbard. *Studia Geologica Polonica* 116: 111–137.

KRAJEWSKI K.P. 2000d. Phosphorus concentration and organic carbon preservation in the Blanknuten Member (Botneheia Formation, Middle Triassic) in Sassenfjorden, Spitsbergen. *Studia Geologica Polonica* 116: 139–173.

KRAJEWSKI K.P. 2000e. Phosphorus and organic carbon reservoirs in the Bravaisberget Formation (Middle Triassic) in Horsund. *Studia Geologica Polonica* 116: 175–209.

KRAJEWSKI K.P. 2013. Organic matter-apatite-pyrite relationships in the Botneheia Formation (Middle Triassic) of eastern Svalbard: Relevance to the formation of petroleum source rocks in the NW Barents Sea shelf. *Marine and Petroleum Geology* 45: 69–105.

KRAJEWSKI K.P., KARCZ P., WOŹNY E. and MØRK A. 2007. Type section of the Bravaisberget Formation (Middle Triassic) at Bravaisberget, western Nathorst Land, Spitsbergen, Svalbard. *Polish Polar Research* 28: 79–122.

KRISTENSEN E., AHMED S.I. and DEVOL A.H. 1995. Aerobic and anaerobic decomposition of organic matter in marine sediment: Which is fastest? *Limnology and Oceanography* 40: 1430–1437.

LANGFORD F.F. and BLANC-VALLERON M.M. 1990. Interpreting Rock-Eval pyrolysis data using graphs and pyrolyzable hydrocarbons vs. total organic carbon. *American Association Petroleum Geologists Bulletin* 74: 799–804.

MARTIN W.R. and BENDER M.L. 1988. The variability of benthic fluxes and sedimentary remineralization rates in response to seasonally variable organic carbon rain rates in the deep sea: A modeling study. *American Journal of Science* 288: 541–574.

MIDDELBURG J.J. 1989. A simple rate model for organic matter decomposition in marine sediments. *Geochimica et Cosmochimica Acta* 53: 1577–1581.

MØRK A. and BROMLEY R.G. 2008. Ichnology of a marine regressive system tract: the Middle Triassic of Svalbard. *Polar Research* 27: 339–359.

MØRK A., EMBRY A.F. and WEITSCHAT W. 1989. Triassic transgressive-regressive cycles in the Sverdrup Basin, Svalbard and the Barents Shelf. *In*: J.D. Collinson (ed.) *Correlation in Hydrocarbon Exploration*. Graham and Trotman, London: 113–130.

MØRK A., KNARUD R. and WORSLEY D. 1982. Depositional and diagenetic environments of the Triassic and Lower Jurassic succession of Svalbard *In*: A.F. Embry and H.R. Balkwill (eds) Arctic Geology and Geophysics. *Canadian Society of Petroleum Geologist Memoir* 8: 371–398.

PEDERSEN T.F., SHIMMIELD G.B. and PRICE N.B. 1992. Lack of enhanced preservation of organic matter in sediments under the oxygen minimum on the Oman margin. *Geochimica et Cosmochimica Acta* 56: 545–551.

PETERS K.E., WALTERS C.C. and MOLDOVAN J.M. 2006. *The Biomarker Guide: V. 1 – Biomarkers and Isotopes in the Environment and Human History*. Cambridge University Press, Cambridge: 471 pp.

PRAHL F.G., ETREL J.R., GONI M.A., SPARROW M.A. and EVERSMAYER B. 1994. Terrestrial organic carbon contributions to sediment on the Washington margin. *Geochimica et Cosmochimica Acta* 58: 3035–3084.

RIIS F., LUNDSCHIEN B.A., HØY T., MØRK A. and MØRK M.B.E. 2008. Evolution of Triassic shelf in the northern Barents Sea region. *Polar Research* 27: 318–338.

ROBERT P. 1988. *Organic Metamorphism and Geothermal History*. Elf – Aguitaine and D. Reidel Publishing Company, Dordrecht: 311 pp.

SARI A. and ALIYEV S.A. 2006. Organic geochemical characteristics of the Paleocene–Eocene oil shales in the Nallihan Region, Ankara, Turkey. *Journal of Petroleum Science and Engineering* 53: 123–134.

SCHMOKER J.W. 1994. Volumetric calculation of hydrocarbon generated. *In*: L.B. Magoon and W.G. Dow (eds) 1994. The Petroleum System – from Source to Trap. *American Association Petroleum Geologists Memoir* 60: 323–326.

SCHOU L., MØRK A. and BJORØY M. 1984. Correlation of source rocks and migrated hydrocarbons by GC-MS in the middle Triassic of Svalbard. *Organic Geochemistry* 6: 513–520.

STEEL R.J. and WORSLEY D. 1984. Svalbard's post Caledonian strata – an atlas of sedimentational patterns and paleogeographic evolution. *In*: A.M. Spencer *et al.* (eds) *Petroleum Geology of the North European Margin*. Norwegian Petroleum Society, Graham and Trotman, London: 109–135.

SUESS E., KULM L.D. and KILLINGLEY J.S. 1987. Coastal upwelling and a history of organic-rich mudstone deposition off Peru. *In*: J. Brooks and A.J. Fleet (eds) *Marine Petroleum Source Rocks: Geological Society Special Publications* 26. Blackwell Scientific Publications, London: 181–197.

WEISNER M.G., HAAKE B. and WIRTH H. 1990. Organic facies of surface sediments in the North Sea. *Organic Geochemistry* 15: 419–432.

Received 11 April 2013
Accepted 14 February 2014